



Published in final edited form as:

*Biochem Pharmacol.* 2006 February 14; 71(4): 540–549. doi:10.1016/j.bcp.2005.11.010.

## Structure activity and molecular modeling analyses of ribose- and base-modified uridine 5'-triphosphate analogues at the human P2Y<sub>2</sub> and P2Y<sub>4</sub> receptors

Kenneth A. Jacobson<sup>a,\*</sup>, Stefano Costanzi<sup>b</sup>, Andrei A. Ivanov<sup>a</sup>, Susanna Tchilibon<sup>a</sup>, Pedro Besada<sup>a</sup>, Zhan-Guo Gao<sup>a</sup>, Savitri Maddileti<sup>c</sup>, and T. Kendall Harden<sup>c</sup>

<sup>a</sup>Molecular Recognition Section, Laboratory of Bioorganic Chemistry, National Institute of Diabetes and Digestive and Kidney Diseases, National Institutes of Health, Bethesda, MD 20892, USA

<sup>b</sup>Computational Chemistry Core Laboratory, National Institute of Diabetes and Digestive and Kidney Diseases, National Institutes of Health, Bethesda, MD 20892, USA

<sup>c</sup>Department of Pharmacology, University of North Carolina School of Medicine, Chapel Hill, NC 27599, USA

### Abstract

With the long-term goal of developing receptor subtype-selective high affinity agonists for the uracil nucleotide-activated P2Y receptors we have carried out a series of structure activity and molecular modeling studies of the human P2Y<sub>2</sub> and P2Y<sub>4</sub> receptors. UTP analogues with substitutions in the 2'-position of the ribose moiety retained capacity to activate both P2Y<sub>2</sub> and P2Y<sub>4</sub> receptors. Certain of these analogues were equieffective for activation of both receptors whereas 2'-amino-2'-deoxy-UTP exhibited higher potency for the P2Y<sub>2</sub> receptor and 2'-azido-UTP exhibited higher potency for the P2Y<sub>4</sub> receptor. 4-Thio substitution of the uracil base resulted in a UTP analogue with increased potency relative to UTP for activation of both the P2Y<sub>2</sub> and P2Y<sub>4</sub> receptors. In contrast, 2-thio substitution and halo- or alkyl substitution in the 5-position of the uracil base resulted in molecules that were 3–30-fold more potent at the P2Y<sub>2</sub> receptor than P2Y<sub>4</sub> receptor. 6-Aza-UTP was a P2Y<sub>2</sub> receptor agonist that exhibited no activity at the P2Y<sub>4</sub> receptor. Stereoisomers of UTPαS and 2'-deoxy-UTPαS were more potent at the P2Y<sub>2</sub> than P2Y<sub>4</sub> receptor, and the R-configuration was favored at both receptors. Molecular docking studies revealed that the binding mode of UTP is similar for both the P2Y<sub>2</sub> and P2Y<sub>4</sub> receptor binding pockets with the most prominent dissimilarities of the two receptors located in the second transmembrane domain (V90 in the P2Y<sub>2</sub> receptor and I92 in the P2Y<sub>4</sub> receptor) and the second extracellular loop (T182 in the P2Y<sub>2</sub> receptor and L184 in the P2Y<sub>4</sub> receptor). In summary, this work reveals substitutions in UTP that differentially affect agonist activity at P2Y<sub>2</sub> versus P2Y<sub>4</sub> receptors and in combination with molecular modeling studies should lead to chemical synthesis of new receptor subtype-selective drugs.

## Keywords

Structure activity relationship; G protein-coupled receptor; Nucleotides; Phospholipase C; Pyrimidines; Homology modeling

---

## 1. Introduction

Pharmacological effects of UTP (uridine 5'-triphosphate) and other uracil nucleotides on second messenger signaling pathways and on various tissue responses provided the initial indications of the existence of cell surface receptors that specifically recognize extracellular pyrimidines [1,2]. This concept was confirmed and extended over the past decade with the cloning of three different G protein-coupled receptors, the P2Y<sub>2</sub>, P2Y<sub>4</sub> and P2Y<sub>6</sub> receptors [3–6] that are activated by uracil nucleotides, and by the direct demonstration of regulated release of UTP from a variety of cell types [7,8].

The P2Y<sub>2</sub> receptor is activated equipotently by both UTP and ATP (adenosine 5'-triphosphate) and is distributed in a broad range of tissues. For example, this receptor plays important physiological roles in epithelial cells of the lung, gastrointestinal tract, eye, and other tissues [9,10]. The human P2Y<sub>4</sub> receptor is selectively activated by UTP, and ATP is a potent competitive antagonist at this receptor [11]. However, the P2Y<sub>4</sub> receptor of several other species is activated by both UTP and ATP [11–13], and therefore, it has proven difficult to differentiate the P2Y<sub>4</sub> receptor from the P2Y<sub>2</sub> receptor on the basis of its cognate agonists in, for example, rat and mouse tissues. The P2Y<sub>6</sub> receptor is selectively activated by UDP (uridine 5'-diphosphate), and UTP is a weak agonist or inactive at this receptor [6,14].

The existence of three different G protein-coupled receptors that recognize uracil nucleotides has made difficult the pharmacological characterization or selective activation of these receptors in native tissues. As has proved to be the case with the P2Y receptors, i.e. P2Y<sub>1</sub>, P2Y<sub>11</sub>, P2Y<sub>12</sub>, and P2Y<sub>13</sub> receptors, that are activated by adenine nucleotides, the metabolism and interconversion of extracellular nucleotides add complexities to the study of uracil nucleotide-activated receptors in native tissues [15]. For example, the ectonucleoside triphosphate diphosphohydrolase, NTPDase2, converts extracellular UTP to UDP [16], whereas ectonucleoside diphosphokinase forms UTP from UDP with the transfer of the  $\gamma$ -phosphate from ATP [17].

Drugs that selectively activate or block the uracil nucleotide-activated P2Y receptors would provide armamentaria for circumvention of some of the problems inherent in the study of these physiologically important signaling proteins. However, receptor subtype-selective agonists or antagonists are not available for the uracil nucleotide-activated P2Y receptors [18]. Therefore, we have undertaken a series of pharmacological studies designed to systematically evaluate the effects of various modifications of the UTP structure on the capacity of analogues to activate the UTP-activated P2Y<sub>2</sub> and P2Y<sub>4</sub> receptors. Since UTP activates the human P2Y<sub>2</sub> and P2Y<sub>4</sub> receptors with similar potencies, our first goal is to identify substitutions in UTP analogues that differentially affect activity at either of these receptors. Conversely, identification of partial agonists at these receptors would open a path to synthesis of selective high affinity antagonists of the UTP-activated P2Y receptors in a

manner similar to the approach we have followed to identify a subnanomolar affinity antagonist for the ADP-activated P2Y<sub>1</sub> receptor [19–21]. The results reveal encouraging progress in the first of these goals. We also conducted docking studies with rhodopsin-based homology models of the P2Y<sub>2</sub> and P2Y<sub>4</sub> receptors with the goal of extending insight gained from the empirical structure activity studies to predict optimized structures that will be pursued by application of new molecular syntheses. The combination of these structure activity analyses and molecular modeling studies provides resolution of key differences in the ligand binding pockets of the P2Y<sub>2</sub> versus P2Y<sub>4</sub> receptor that will be of heuristic importance for future ligand development.

## 2. Materials and methods

### 2.1. Reagents

2'-Ara-fluoro-2'-deoxyuridine (**25**) was purchased from R.I. Chemical, Inc. (Orange, CA). All other reagents and solvents were purchased from Sigma–Aldrich (St. Louis, MO).

### 2.2. Uracil nucleotide analogues

Most of the nucleotide analogues studied (compounds **5–10**, **12–17**, and **20**) were purchased from TriLink Biotechnologies (San Diego, CA). Compound **19** was custom synthesized by TriLink Biotechnologies and was the gift of Dr. Victor Marquez, NCI, Frederick, MD. Compounds **1–4** and 3-methyluridine (**26**) were purchased from Sigma (St. Louis, MO). Compounds **21–24** were manufactured by Axxora (San Diego, CA)/Biolog Life Science Inst. (Bremen, Germany).

### 2.3. Chemical synthesis

**2.3.1. Chemical methods**—Methods used to prepare compounds **11** and **18** are depicted schematically in Fig. 1. <sup>1</sup>H NMR spectra were obtained with a Varian Gemini 300 spectrometer using D<sub>2</sub>O as a solvent. The chemical shifts are expressed as relative ppm from HOD (4.78 ppm). <sup>31</sup>P NMR spectra were recorded at room temperature by use of Varian XL 300 spectrometer (121.42 MHz); orthophosphoric acid (85%) was used as an external standard. Purity of compounds was checked using a Hewlett-Packard 1100 HPLC equipped with a Luna 5μ RP-C18(2) analytical column (250 mm × 4.6 mm; Phenomenex, Torrance, CA). System A—linear gradient solvent system: 5 mM TBAP-CH<sub>3</sub>CN from 80:20 to 40:60 in 20 min, then isocratic for 2 min; the flow rate was 1 mL/min. System B—linear gradient solvent system: 10 mM TEAA-CH<sub>3</sub>CN from 100:0 to 90:10 in 20 min, then isocratic for 2min; the flow rate was 1 mL/min. Peaks were detected by UV absorption with a diode array detector. All derivatives tested for biological activity showed >99% purity in the HPLC systems. High-resolution mass measurements were performed on Micromass/Waters LCT Premier Electrospray Time of Flight (TOF) mass spectrometer coupled with a Waters HPLC system. Purification of the nucleotide analogues for biological testing was carried out on (diethylamino)ethyl (DEAE)-A25 Sephadex columns with a linear gradient (0.01–0.5 M) of 0.5 M ammonium bicarbonate as the mobile phase. Compounds **27** and **28** were additionally purified by HPLC using system C (10 mM TEAA-CH<sub>3</sub>CN from 100:0 to 90:10 in 30 min, then isocratic for 2 min; the flow rate was 2 mL/min) with a Luna 5μ RP-C18(2) semipreparative column (250 mm × 10.0 mm; Phenomenex, Torrance, CA).

### 2.3.2. General procedure for preparation of nucleoside 5'-triphosphate

**(compound 18)**—3-Methyluridine (**26**) (25 mg, 0.10 mmol) and Proton Sponge (31 mg, 0.15 mmol) were dried for several hours in high vacuum and then dissolved in trimethyl phosphate (1 mL). After cooling the solution at 0 °C, phosphorous oxychloride (0.02 mL, 0.19 mmol) was added. The mixture reaction was stirred at 0 °C for 2 h. A solution of tributylammonium pyrophosphate (303 mg, 0.64 mmol) and tributylamine (0.09 mL, 0.39 mmol) in DMF (1 mL) was added and stirring was continued at 0 °C for additional 20 min. Five milliliters of 0.2 M triethylammonium bicarbonate (TEAB) solution was added, and the reaction mixture was stirred at room temperature for 45 min. Analysis of the reaction mixture by analytical HPLC (System A) indicated the formation of three compounds, the corresponding nucleotide mono-, di-, and triphosphates. The mixture was subsequently frozen and lyophilized, and the residue was purified by Sephadex-DEAE A-25 resin ion-exchange column chromatography and when was necessary (compounds **27** and **28**) by semipreparative HPLC as described above. The corresponding nucleotide mono-, di-, and triphosphates were collected, frozen, and lyophilized as the triethylammonium or ammonium salts. (2'*R*,3'*R*,4'*S*,5'*R*)-1-(3',4'-dihydroxy-5'-phosphoryloxymethyltetrahydrofuran-2'-yl)-3-methyl-1H-pyrimidine-2,4-dione, triethylammonium salt (**27**) was obtained as a white solid (6 mg, 11%). <sup>1</sup>H NMR (D<sub>2</sub>O) δ 8.06 (d, *J* = 8.4 Hz, 1H), 6.04 (d, *J* = 8.1 Hz, 1H), 6.02 (d, *J* = 4.2 Hz, 1H), 4.37 (m, 2H), 4.28 (m, 1H), 4.07 (m, 2H), 3.30 (s, 3H); <sup>31</sup>P NMR (D<sub>2</sub>O) δ 1.88; HRMS *m/z* found 337.0404 (*M* – H<sup>+</sup>)<sup>-</sup>. C<sub>10</sub>H<sub>14</sub>N<sub>2</sub>O<sub>9</sub>P requires 337.0437; HPLC (System A) 7.6 min (99%), (System B) 11.5 min (99%). (2'*R*,3'*R*,4'*S*,5'*R*)-1-(3',4'-dihydroxy-5'-diphosphoryloxymethyltetrahydrofuran-2'-yl)-3-methyl-1H-pyrimidine-2,4-dione, triethylammonium salt (**28**) was obtained as a white solid (1 mg, 1%). <sup>1</sup>H NMR (D<sub>2</sub>O) δ 8.01 (d, *J* = 7.8 Hz, 1H), 6.05 (d, *J* = 8.1 Hz, 1H), 6.01 (d, *J* = 3.6 Hz, 1H), 4.41 (m, 2H), 4.27 (m, 3H), 3.31 (s, 3H); <sup>31</sup>P NMR (D<sub>2</sub>O) δ –8.68, –11.32 (d, *J* = 21.4 Hz); HRMS *m/z* found 417.0116 (*M* – H<sup>+</sup>)<sup>-</sup>. C<sub>10</sub>H<sub>15</sub>N<sub>2</sub>O<sub>12</sub>P<sub>2</sub> requires 417.0100; HPLC (System A) 14.3 min (99%), (System B) 12.4 min (99%). (2'*R*,3'*R*,4'*S*,5'*R*)-1-(3',4'-dihydroxy-5'-triphosphoryloxymethyl-tetrahydrofuran-2'-yl)-3-methyl-1H-pyrimidine-2,4-dione, ammonium salt (**18**) was obtained as a white solid (8 mg, 15%). <sup>1</sup>H NMR (D<sub>2</sub>O) δ 7.98 (d, *J* = 8.1 Hz, 1H), 6.02 (m, 2H), 4.44 (m, 1H), 4.40 (m, 1H), 4.28 (m, 3H), 3.29 (s, 3H); <sup>31</sup>P NMR (D<sub>2</sub>O) δ –6.64 (d, *J* = 20.2 Hz), –10.88 (d, *J* = 19.5 Hz), –21.91 (t, *J* = 20.2 Hz); HRMS *m/z* found 496.9750 (*M* – H<sup>+</sup>)<sup>-</sup>. C<sub>10</sub>H<sub>16</sub>N<sub>2</sub>O<sub>15</sub>P<sub>3</sub> requires 496.9764; HPLC (System A) 18.3 min (99%), (System B) 13.5 min (99%).

(2'*R*,3'*S*,4'*S*,5'*R*)-1-(3'-Fluoro-4'-hydroxy-5'-triphosphoryloxymethyl-tetrahydrofuran-2'-yl)-1H-pyrimidine-2,4-dione, ammonium salt (**11**). Compound **11** (29 mg, 26%) was obtained as a white solid from 2'-ara-fluoro-2'-deoxyuridine (**25**) following the general procedure for **18**. <sup>1</sup>H NMR (D<sub>2</sub>O) δ 7.93 (d, *J* = 8.1 Hz, 1H), 6.34 (d, *J* = 15.6 Hz, 1H), 5.94 (d, *J* = 8.1 Hz, 1H), 5.24 (d, *J* = 51.6 Hz, 1H), 4.60 (d, *J* = 19.5 Hz, 1H), 4.25 (m, 3H); <sup>31</sup>P NMR (D<sub>2</sub>O) δ –9.86, –11.46 (d, *J* = 19.6 Hz), –23.05; HRMS *m/z* found 484.9576 (*M* – H<sup>+</sup>)<sup>-</sup>. C<sub>9</sub>H<sub>13</sub>N<sub>2</sub>O<sub>14</sub>FP<sub>3</sub> requires 484.9564; HPLC (System A) 19.0 min (99%), (System B) 11.6 min (99%).

#### 2.4. Assay of P2Y<sub>2</sub> and P2Y<sub>4</sub> receptor-stimulated phospholipase C activity

Stable cell lines expressing the human P2Y<sub>2</sub> receptor or the human P2Y<sub>4</sub> receptor in 1321N1 human astrocytoma cells were generated as previously described in detail [14]. Agonist-induced [<sup>3</sup>H]inositol phosphate production was measured in 1321N1 cells grown to confluence on 48-well plates. Twelve hours before the assay, the inositol lipid pool of the cells was radiolabeled by incubation in 200 μL of serum-free inositol-free Dulbecco's modified Eagle's medium, containing 0.4 μCi of *myo*-[<sup>3</sup>H]inositol. No changes of medium were made subsequent to the addition of [<sup>3</sup>H]inositol. On the day of the assay, cells were challenged with 50 μL of the five-fold concentrated solution of receptor agonists in 200 mM Hepes, pH 7.3, containing 50 mM LiCl for 20 min at 37 °C. Incubations were terminated by aspiration of the drug-containing medium and addition of 450 μL of ice-cold 50 mM formic acid. After 15 min at 4 °C, samples were neutralized with 150 μL of 150 mM NH<sub>4</sub>OH. [<sup>3</sup>H]Inositol phosphates were isolated by ion exchange chromatography on Dowex AG 1-X8 columns as previously described [22].

#### 2.5. Data analyses

Agonist potencies (EC<sub>50</sub> values) were obtained from concentration–response curves by non-linear regression analysis using the GraphPad software package Prism (GraphPad, San Diego, CA). All experiments were performed in triplicate assays and repeated at least three times. The results are presented as mean ± S.E.M. from multiple experiments or in the case of concentration effect curves from a single experiment carried out with triplicate assays that were representative of results from multiple experiments.

#### 2.6. Reconstruction of the binding pocket model

The reconstruction of the P2Y<sub>2</sub> and P2Y<sub>4</sub> receptors around UTP was performed with the InducedFit module of the Prime 1.2 homology modeling program (Schrödinger, LLC). The calculation was restricted to the residues located within 5 Å of the ligand.

#### 2.7. Conformational analysis of UTP inside the putative binding pocket

A conformational analysis of UTP in the binding pockets of the P2Y<sub>2</sub> and P2Y<sub>4</sub> receptors was performed by means of the mixed MCMM/LMCS sampling method as implemented in Macro-Model 9.0 [23] (Schrödinger, LLC). The approach combines the Monte Carlo Multiple Minimum (MCMM) [24] and the low-mode conformational search (LMCS) [25]. All of the rotatable bonds of the ligand, as well as the ligand itself as a single body, were subjected to Monte Carlo driven rotations and translations during the conformational search. The search was performed on the ligand and the residues located within 5 Å of the ligand, while the remaining residues were conformationally frozen. The calculations were conducted with the MMFFs force field [26], using water as implicit solvent (GB/SA model [27] as implemented in MacroModel [23]) and a molecular dielectric constant of 1. The Polak-Ribier Conjugate Gradient was used for the energy minimizations with a convergence threshold of 0.05 kJ/mol/Å.

### 3. Results

#### 3.1. Chemical synthesis

Synthetic methods for the preparation of nucleoside 5'-triphosphate derivatives **11** and **18** from the nucleosides of **25** and **26**, respectively, are shown in Fig. 1. The classical phosphorous oxychloride method was used for the synthesis of both derivatives [28,29]. The 5'-mono (**27**) and diphosphate (**28**) derivatives of **26** were also isolated as side products.

#### 3.2. Pharmacological assays and structure activity relationships

The human P2Y<sub>2</sub> and P2Y<sub>4</sub> receptors were stably expressed in 1321N1 human astrocytoma cells using retroviral vectors as previously described [14]. Agonist-promoted activation of phospholipase C (PLC) was assessed in these two stable cell lines by quantification of the accumulation of [<sup>3</sup>H]inositol phosphates as described in Section 2. UTP markedly stimulated [<sup>3</sup>H]inositol phosphate accumulation to similar levels in P2Y<sub>2</sub> versus P2Y<sub>4</sub> receptor-expressing cells. Similar EC<sub>50</sub> values also were observed for UTP (**1**) for activation of the two receptors (Fig. 2 and Table 1). ATP (**2**) was two-fold less potent than UTP at the human P2Y<sub>2</sub> receptor, and CTP (**3a**) and GTP (**3b**) were only weakly active at this subtype. Both nucleotides were previously shown to be antagonists at the human P2Y<sub>4</sub> receptor [11].

Given the similar activities of UTP at the P2Y<sub>2</sub> versus P2Y<sub>4</sub> receptor, we compared the activities of a series of ribose-modified UTP analogues (**4–11**) for activation of the two receptor types. Although less potent than UTP in most cases, all 2'-substituted molecules retained capacity to maximally stimulate both receptors in the test system used. Whereas similar potencies were observed for the 2'-*O*-methyl-substituted (**5**) and 2'-fluoro-substituted (**9**) molecules at the P2Y<sub>2</sub> versus P2Y<sub>4</sub> receptors (Table 1), differential effects on potencies at the two receptors were observed with 2'-amino (**7**) and 2'-azido (**8**) substitutions (Fig. 2 and Table 1). That is, the potency of 2'-amino-2'-deoxyuridine-5'-triphosphate (**7**) was unchanged from UTP at the P2Y<sub>2</sub> receptor but was 16-fold less at the P2Y<sub>4</sub> receptor. Conversely, 2'-azido-substitution in **8** resulted in a greater decrease in potency at the P2Y<sub>2</sub> receptor than at the P2Y<sub>4</sub> receptor. Interestingly, existence of the 2'-hydroxyl of UTP in the arabino configuration in **10** resulted in a molecule that exhibits similar potency to UTP at the P2Y<sub>2</sub> receptor but 10-fold reduced potency at the P2Y<sub>4</sub> receptor. The only 3'-substituted molecule, 3'-*O*-methyluridine-5'-triphosphate (**6**), tested was inactive at both P2Y<sub>2</sub> and P2Y<sub>4</sub> receptors.

Uracil-substituted UTP analogues (**12–20**) also were examined. Modification of UTP with a thio moiety in the 4 position in **16** resulted in an analogue that was two-fold and three-fold more potent than UTP at the P2Y<sub>2</sub> and P2Y<sub>4</sub> receptors, respectively (Fig. 3 and Table 1). In contrast, 2-thio-substitution in **15** resulted in a molecule that was at least as potent as UTP at the P2Y<sub>2</sub> receptor and 5-fold less potent at the P2Y<sub>4</sub> receptor. Halo- or alkyl substitution in the 5-position of the base (**12–14**) resulted in molecules 3–10-fold more potent at the P2Y<sub>2</sub> receptor than the P2Y<sub>4</sub> receptor. Aza-substitution in the 6-position in **17** decreased potency at the P2Y<sub>2</sub> receptor and resulted in an analogue that was inactive at the P2Y<sub>4</sub> receptor. A decrease in P2Y<sub>2</sub> receptor potency and complete loss of activity at the P2Y<sub>4</sub> receptor also occurred with replacement of uracil with a pyrimidinone ring moiety, i.e. zebularine-5'-

triphosphate [30]. Conversely, attenuated agonist activity was observed at the P2Y<sub>2</sub> and P2Y<sub>4</sub> receptors with pseudouridine-5'-triphosphate (**20**), in which the base moiety is replaced with a reoriented uracil ring.

Phosphate side chain modification as phosphothioates was examined in the stereoisomers of UTP $\alpha$ S and 2'-deoxy-UTP $\alpha$ S (**21–24**). These phosphate side chain modifications decreased agonist potency by approximately two orders of magnitude. Both stereoisomers of UTP $\alpha$ S (**21, 22**) were approximately fivefold more potent at the P2Y<sub>2</sub> receptor than the P2Y<sub>4</sub> receptor (Fig. 4 and Table 1). The R-configuration was favored by both receptors by approximately three-fold over the S-isomer. R<sub>p</sub>-2'-deoxy-UTP $\alpha$ S (**23**), although displaying a relatively large standard error, was a full agonist at the P2Y<sub>2</sub> receptor and inactive at the P2Y<sub>4</sub> receptor. S<sub>p</sub>-2'-deoxy-UTP $\alpha$ S (**24**) was inactive at both the P2Y<sub>2</sub> and P2Y<sub>4</sub> receptors.

### 3.3. Flexible docking of UTP into putative binding pockets of the P2Y<sub>2</sub> and P2Y<sub>4</sub> receptors

We recently proposed, supported by experimental data, a hypothetical binding mode of nucleotides within P2Y receptors of subgroup A (P2Y<sub>1</sub>, P2Y<sub>2</sub>, P2Y<sub>4</sub>, P2Y<sub>6</sub>, and P2Y<sub>11</sub>) [31,32]. Briefly, the cognate agonist nucleotide of each of these receptors is accommodated in the cavity defined by the third, sixth, and seventh transmembrane domains (TM) and the second extracellular loop (EL2). The ribose moiety of agonists is located between TM3 and TM7, with the negatively charged phosphate groups pointing toward TM6 and the nucleobase pointing toward TM1 and TM2.

Our previous success in identification of new receptor-selective high affinity agonists and antagonists of the P2Y<sub>1</sub> receptor [19–21,33] was driven in part by a close interplay of structure activity analyses, rational new drug syntheses, and molecular modeling of the P2Y<sub>1</sub> receptor binding site. Thus, we have carried out new modeling studies as described in Section 2 to further refine insight into the binding pocket of the P2Y<sub>2</sub> and P2Y<sub>4</sub> receptors. Our previously published binding mode [31,32] was utilized to position UTP in the putative binding pockets of the unoccupied P2Y<sub>2</sub> and P2Y<sub>4</sub> receptors. These respective binding pockets then were reconstructed around docked UTP by means of homology modeling under conditions that allowed the receptors to adapt to the presence of ligand. We subsequently performed a concerted conformational analysis of UTP and the surrounding residues, exploring simultaneously the flexibility of the ligand and the receptors. To facilitate the comparison among receptors, throughout this paper we use the GPCR residue indexing system, as explained in detail elsewhere [31].

The putative nucleotide binding pockets of the P2Y<sub>2</sub> and P2Y<sub>4</sub> receptors are highly conserved and, not surprisingly, the results of our docking experiments indicated very similar binding modes of UTP within both receptors (Fig. 5). The most prominent dissimilarities between the putative UTP binding pockets in the P2Y<sub>2</sub> and P2Y<sub>4</sub> receptors were found in residues located in TM2 (V90(2.61) in the P2Y<sub>2</sub> receptor corresponding to I92(2.61) in the P2Y<sub>4</sub> receptor) and a residue in EL2 (T182 in the P2Y<sub>2</sub> receptor corresponding to L184 in P2Y<sub>4</sub> receptor). Both of these non-conserved residues are located in proximity to the uracil moiety of UTP, and their presence results in an apparently smaller binding pocket of the P2Y<sub>4</sub> receptor for the cognate agonist.

The docking models suggested other ligand recognition elements. In agreement with observations for the P2Y<sub>1</sub> receptor [31,32], the triphosphate moiety of UTP is putatively coordinated by three conserved cationic residues (Fig. 5). These residues, all Arg in P2Y<sub>2</sub> and P2Y<sub>4</sub> receptors, are located in TM3 (3.29), TM6 (6.55), and TM7 (7.39). A fourth cationic residue located at the 7.36 position is in proximity to the ligand but, consistent with mutagenesis data [34], apparently does not directly interact. The NH at the 3-position of the uracil ring donates an H-bond to a Ser in TM7 (7.43). Alternatively, in other docking poses Ser(7.43) donated an H-bond to the oxygen at the 2-position of the uracil ring. This Ser residue is highly conserved within the P2Y family. Mutagenesis data revealed its fundamental role in the recognition of agonists and antagonists at the P2Y<sub>1</sub> receptor, where it is probably involved in the coordination of the adenine base [31].

#### 4. Discussion

Results from this study provide the first systematic structure activity analysis designed to distinguish the P2Y<sub>2</sub> versus P2Y<sub>4</sub> receptor selectivity of base- and ribose-modified analogues of UTP. The UTP receptor selectivity of molecules with phosphate side chain modified UTP, i.e. stereoisomers of UTP $\alpha$ S and 2'-deoxy-UTP $\alpha$ S, also was examined. Thio-substitution at the 4-position increases potency at both P2Y<sub>2</sub> and P2Y<sub>4</sub> receptors, whereas other base- or ribose-modifications were identified that differentially affect the capacity of analogues to activate the P2Y<sub>2</sub> versus P2Y<sub>4</sub> receptor. These results lay the ground-work for rational drug synthesis directed at generation of high affinity agonists that selectively activate either the P2Y<sub>2</sub> receptor or P2Y<sub>4</sub> receptor.

The P2Y<sub>2</sub> receptor is broadly distributed in mammalian tissues, and its expression in epithelial cells of the lung, eye, and other tissues make it a potentially important therapeutic target in cystic fibrosis, eye disease, and other pathophysiologies [9,10]. Although the P2Y<sub>4</sub> receptor is less prominent than the P2Y<sub>2</sub> receptor in mammals, the presence of this signaling protein on neuronal, vascular, and epithelial tissues also makes the P2Y<sub>4</sub> receptor a potentially important drug target. Simultaneous expression of P2Y<sub>2</sub> and P2Y<sub>4</sub> receptors occurs in a number of cell types and tissues. These receptors theoretically can be delineated in human tissues since whereas both UTP and ATP activate the human P2Y<sub>2</sub> receptor, only UTP activates the human P2Y<sub>4</sub> receptor. However, both of these receptors are potently activated by ATP and UTP in rodents [11–13], and the complexities introduced by metabolism and interconversion of nucleotides also makes pharmacological delineation of the P2Y<sub>2</sub> and P2Y<sub>4</sub> receptors difficult in human tissues using the natural triphosphate agonists [15].

Few studies have addressed selectivity of synthetic nucleotide analogues at the P2Y<sub>2</sub> and P2Y<sub>4</sub> receptors, and no systematic comparison of structure activity relationships has been made for the P2Y<sub>2</sub> receptor versus P2Y<sub>4</sub> receptor using a unified assay system. Certain UTP analogues with substitutions in the 4-position of the base have been reported, and several of these, e.g. 4-*SH* or 4-*S*-hexyl analogues of UTP, retained potencies similar to UTP at the P2Y<sub>2</sub> receptor [35]. To our knowledge the activities of these molecules at the P2Y<sub>4</sub> receptor have not been reported. 5-Br-UTP is an agonist at both P2Y<sub>2</sub> and P2Y<sub>4</sub> receptors, but relative potencies have not been compared simultaneously in the same test system. We











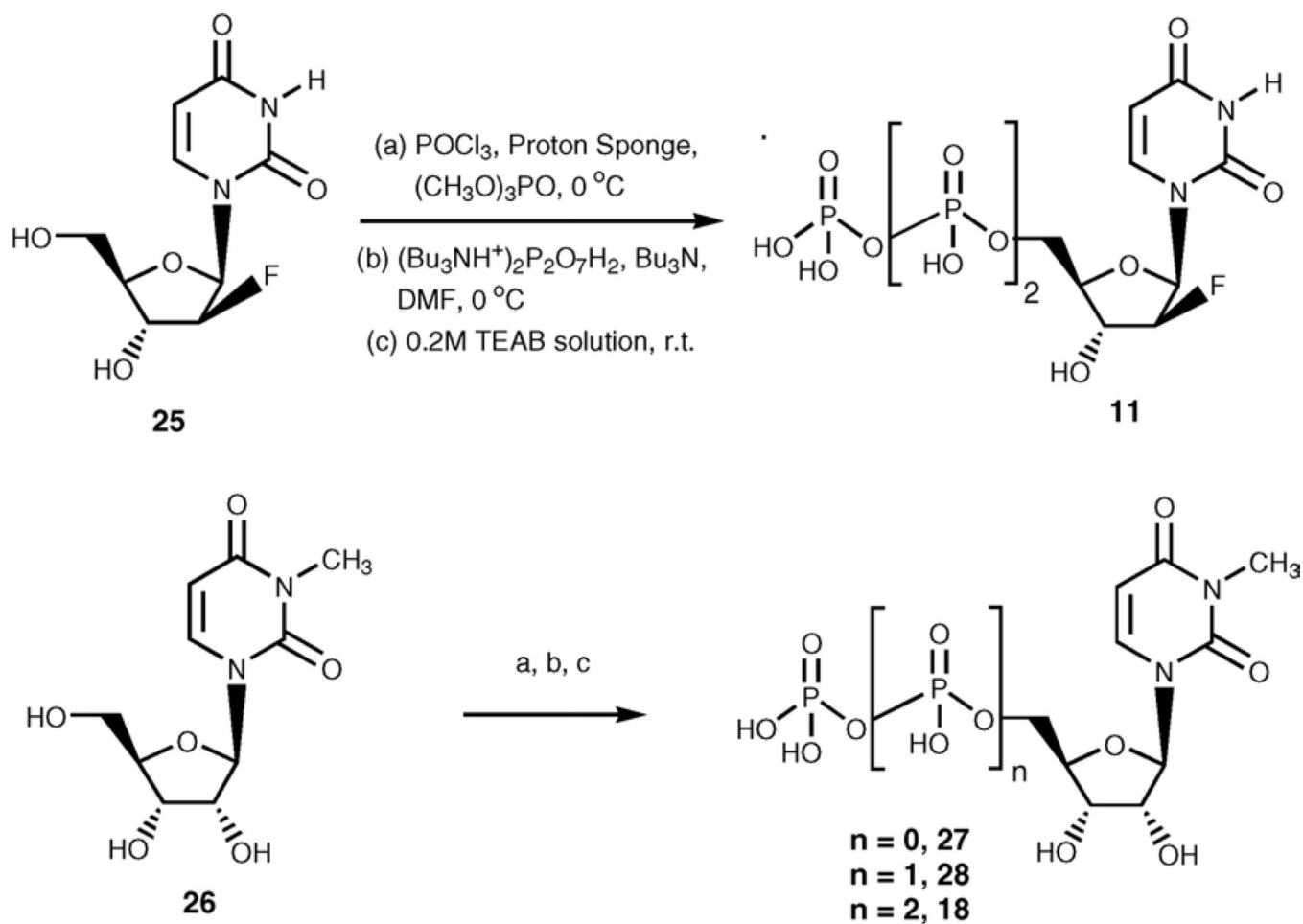


**Fig. 1.**  
Synthetic methods for the preparation of compounds 11 and 18.

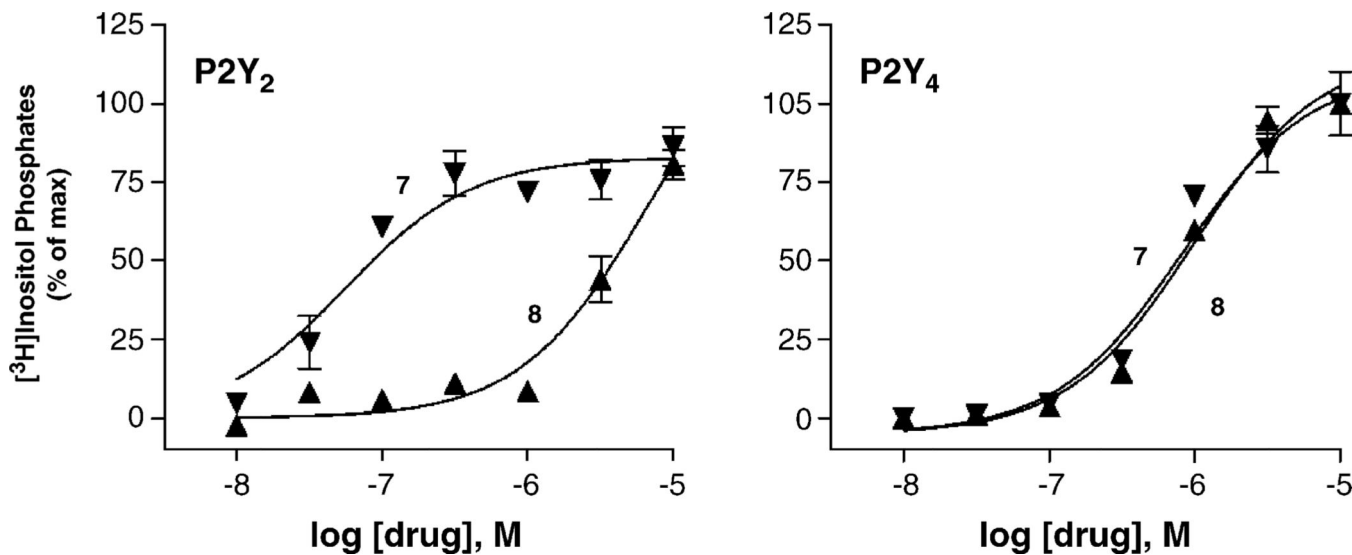


**Fig. 2.** Activation of the human P2Y<sub>2</sub> (left panel), and P2Y<sub>4</sub> (right panel) receptors by ribose-modified uracil 2'-deoxynucleotide analogues containing 2'-amino (7) (▼) and 2'-azido (8) (▲) functionality. PLC activity was measured as described in Section 3.2 in 1321N1 human astrocytoma cells stably expressing the human P2Y receptors. The data are the means of triplicate determinations and are representative of results obtained in at least three separate experiments with each analog.

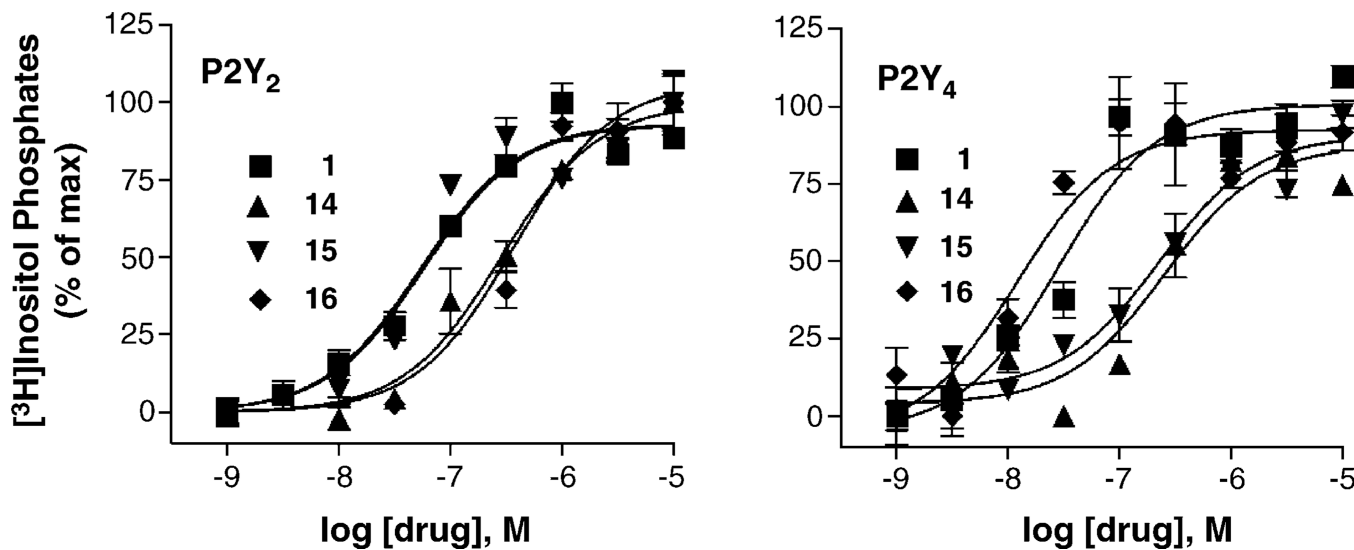


**Fig. 3.**

Activation of the human P2Y<sub>2</sub> (left panel), and P2Y<sub>4</sub> (right panel) receptors by UTP (*1*) and its base-modified uracil nucleotide analogues having 5-methyl (**14**), 2-thio (**15**), and 4-thio (**16**) substitution. PLC activity was measured as described in Section 3.2 in 1321N1 human astrocytoma cells stably expressing the human P2Y receptors. The data are the means of triplicate determinations and are representative of results obtained in at least three separate experiments with each analog.





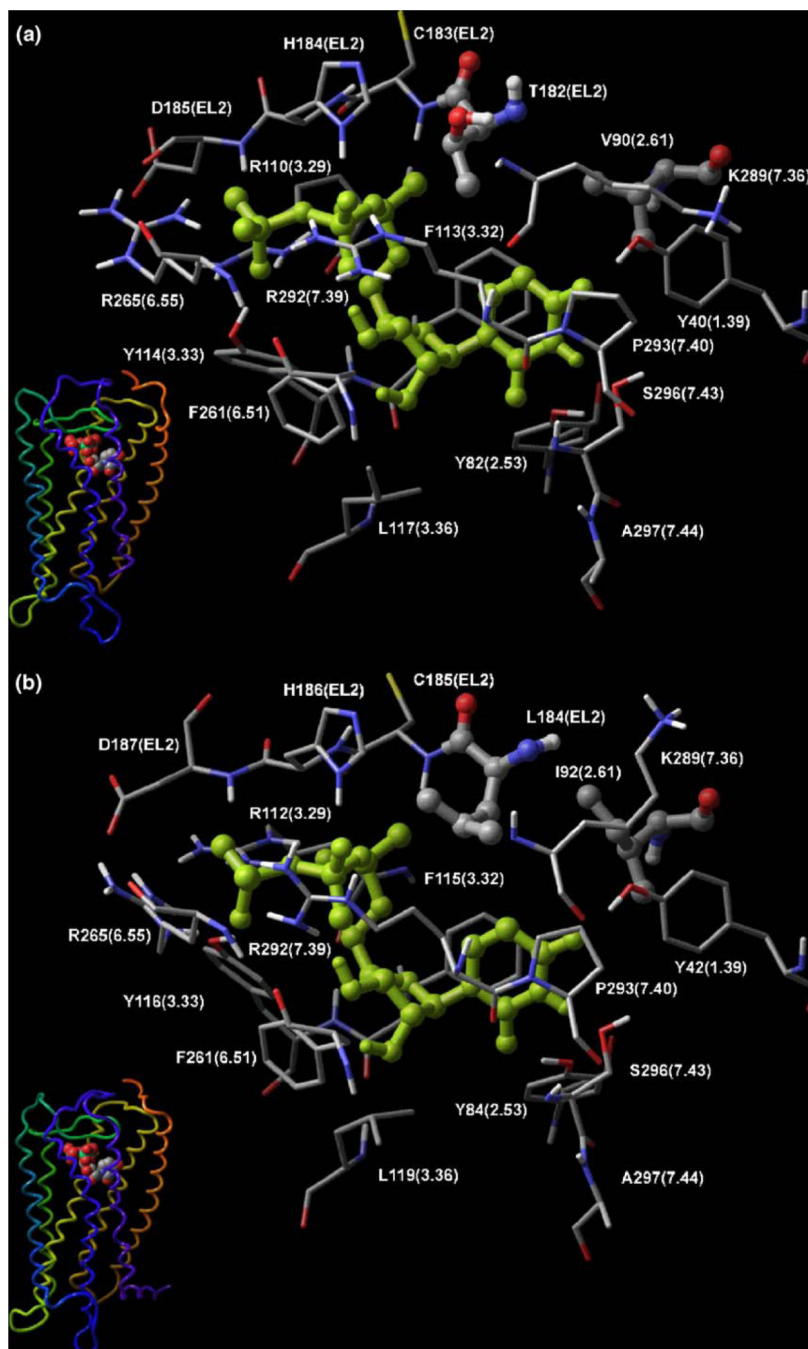


**Fig. 5.** Models of the complexes formed by UTP (*I*) with the P2Y<sub>2</sub> (a) and P2Y<sub>4</sub> (b) receptors. The nucleotide binding pockets are highly conserved in the two receptors [23]. The only two sites of divergence can be found in two residues located in TM2 and EL2 (represented with balls and sticks) in proximity to the uracil-binding pocket. To the left of each detailed binding site is a schematic representation of the entire receptor structure complexed with UTP. In the tube representations the receptor is colored according to residue positions, with a spectrum of colors that ranges from red (N-terminus) to purple (C-terminus): TM1 is in

orange, TM2 in ochre, TM3 in yellow, TM4 in green, TM4 in cyan, TM5 in blue, TM7 in purple.

Author Manuscript

Author Manuscript

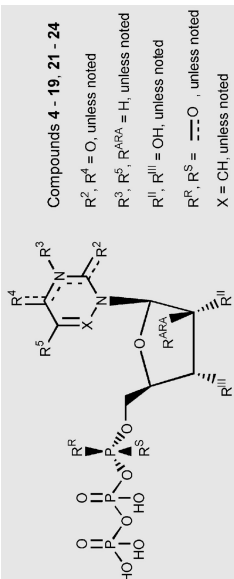
Author Manuscript

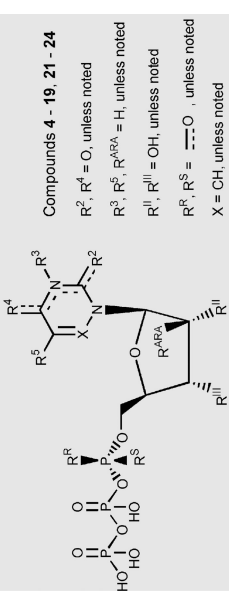
Author Manuscript

In vitro pharmacological data for UTP (1) and its analogues in the stimulation of PLC at recombinant human P2Y<sub>2</sub> and P2Y<sub>4</sub> receptors expressed in astrocytoma cells

**Table 1**

Compound	Modification	Structure	EC <sub>50</sub> at hP2Y <sub>2</sub> receptor (μM) <sup>a</sup>	Relative to UTP	EC <sub>50</sub> at hP2Y <sub>4</sub> receptor (μM) <sup>a</sup>	Relative to UTP
Native ribonucleoside-5'-triphosphates						
1	UTP		0.049 ± 0.012	1	0.073 ± 0.02	1
2	ATP		0.085 ± 0.012	1.7	Antagonist <sup>b</sup>	
3a	CTP		5.63 ± 0.30	110	Antagonist <sup>b</sup>	
3b	GTP		2.64 ± 0.30	54	6.59 <sup>b</sup>	90
Ribose-modified UTP analogues						
4	2'-Deoxy		1.08 ± 0.28	22	1.9 ± 0.5	26
5	2'-Deoxy-2'-methoxy		14.3 ± 7.7	290	8.2 ± 2.1	110
6	3'-Deoxy-3'-methoxy		NE	>1000	NE	>1000
7	2'-Amino-2'-deoxy		0.062 ± 0.008	1.3	1.2 ± 0.3	16
8	2'-Azido-2'-deoxy		5.0 ± 2.1	100	1.1 ± 0.1	15
9	2'-Deoxy-2'-fluoro		0.78 ± 0.11	16	0.54 ± 0.14	7.4
10	Arabino		0.087 ± 0.010	1.8	0.71 ± 0.08	9.7
11	2'-Deoxy-arabino-2'-fluoro-		0.52 ± 0.15	11	0.52 ± 0.08	7.1
Uracil-modified UTP analogues						
12	5-Bromo		0.75 ± 0.1	15	2.1 ± 0.7	29
13	5-Iodo		0.83 ± 0.1	17	4.0 ± 1.7	55





Compounds **4 - 19, 21 - 24**  
 $R^1, R^2, R^3, R^4, R^5 = O$ , unless noted  
 $R^6, R^7, R^8 = H$ , unless noted  
 $R^9, R^{10}, R^{11} = OH$ , unless noted  
 $R^{12}, R^{13} = O$ , unless noted  
 $R^{14}, R^{15} = CH$ , unless noted  
 $X = CH$ , unless noted

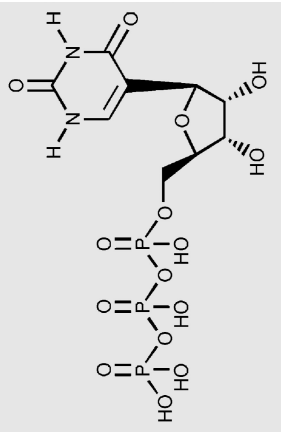
Compound	Modification	Structure	EC <sub>50</sub> at hpP2Y <sub>2</sub> receptor (μM) <sup>a</sup>	Relative to UTP	EC <sub>50</sub> at hpP2Y <sub>4</sub> receptor (μM) <sup>a</sup>	Relative to UTP
<b>14</b>	5-Methyl	$R^5 = CH_3$	$0.48 \pm 0.1$	9.8	$3.9 \pm 1.6$	53
<b>15</b>	2-Thio	$R^2 = S$	$0.035 \pm 0.004$	0.71	$0.35 \pm 0.01$	4.8
<b>16</b>	4-Thio	$R^4 = S$	$0.026 \pm 0.01$	0.53	$0.023 \pm 0.005$	0.32
<b>17</b>	6-Aza	$X = N$	$8.6 \pm 3.7$	180	NE	>1000
<b>18</b>	3-Methyl	$R^3 = CH_3$	$1.20 \pm 0.20$	24	$3.4 \pm 0.8$	47
<b>19</b>	Zebularine analogue	$R^4 = H, H$	$8.9 \pm 0.5$	180	NE	>1000
<b>20</b>	Pseudouridine	<i>c</i>	$0.78 \pm 0.5$	16	$3.0 \pm 0.3$	41
Phosphate-modified UTP analogues						
<b>21</b>	R <sub>p</sub> -α-thio	$R^8 = S$	$5.4 \pm 1.5$	110	$27 \pm 5$	370
<b>22</b>	S <sub>p</sub> -α-thio	$R^8 = S$	$14 \pm 5.5$	290	$81 \pm 8$	1100
<b>23</b>	2'-Deoxy-R <sub>p</sub> -α-thio-triphosphate	$R^8 = S, R^{11} = H$	$12.5 \pm 6.7$	260	NE	>1000
<b>24</b>	2'-Deoxy-S <sub>p</sub> -α-thio triphosphate	$R^8 = S, R^{11} = H$	NE	>1000	NE	>1000

NE: no effect at 10 μM.

<sup>a</sup> Agonist potencies were calculated using a four-parameter logistic equation and the GraphPad software package (GraphPad, San Diego, CA). EC<sub>50</sub> values (mean ± S.E.) represent the concentration at which 50% of the maximal effect is achieved. EC<sub>50</sub> is also expressed relative to the value for UTP at each receptor. Relative efficacies (%) were determined by comparison with the effect produced by a maximal effective concentration of reference agonist (UTP) in the same experiment. For all of the nucleotides, except **22** and **23**, for which an EC<sub>50</sub> is reported in this table, ~100% efficacy was achieved.

<sup>b</sup> ATP antagonized the human P2Y<sub>4</sub> receptor with a  $K_B$  of 0.708 μM. CTP (100 μM) inhibited the response to an EC<sub>50</sub> concentration of UTP by ~40% [11].

<sup>c</sup> Compound **20** has the following structure:



Author Manuscript

Author Manuscript

Author Manuscript

Author Manuscript